JOC The Journal of Organic Chemistry

Featured Article

pubs.acs.org/joc

Recognition of Double-Stranded DNA Using Energetically Activated Duplexes Modified with N2′-Pyrene-, Perylene-, or Coronene-Functionalized 2′-*N*-Methyl-2′-amino-DNA Monomers

Brooke A. Anderson,[†] Jared J. Onley,[†,‡] and Patrick J. Hrdlicka*[,†]

[†]Department of Chemistry, University of Idaho, Moscow, Idaho 83844, United States

[‡]Department of Chemistry, Whitworth University, Spokane, Washington 99251, United States

Supporting Information

ABSTRACT: Invader probes have been proposed as alternatives to polyamides, triplex-forming oligonucleotides, and peptide nucleic acids for recognition of chromosomal DNA targets. These double-stranded probes are activated for DNA recognition by +1 interstrand zippers of pyrene-functionalized nucleotides. This particular motif forces the intercalating pyrene moieties into the same region, resulting in perturbation and destabilization of the probe duplex. In contrast, the two probe strands display very high affinity toward complementary DNA. The energy difference between the probe duplexes and recognition complexes provides the driving force for DNA recognition. In the present study, we explore the properties of Invader probes based on larger intercalators, i.e., perylene and coronene, expecting that the larger π-surface area will result in additional destabilization of the probe duplex and further stabilization of probe−target duplexes, in effect increasing the thermodynamic driving force for DNA recognition. Toward this end, we developed protocols for 2′-*N*-methyl-2′-amino-2′-deoxyuridine phosphoramidites that are functionalized at the N2′-position with pyrene, perylene, or coronene moieties and incorporated these monomers into oligodeoxyribonucleotides (ONs). The resulting ONs and Invader probes are characterized by thermal denaturation experiments, analysis of thermodynamic parameters, absorption and fluorescence spectroscopy, and DNA recognition experiments. Invader probes based on large intercalators efficiently recognize model targets.

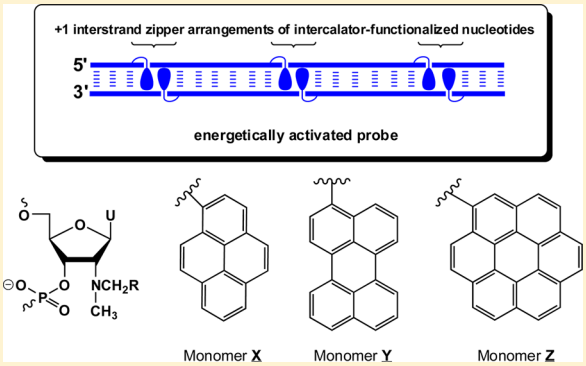

INTRODUCTION

Development of probes for recognition of specific double-stranded DNA (dsDNA) continues to be an area that attracts considerable interest due to the prospect of tools for applications in biological sciences and medicine, including regulation of gene expression via transcriptional interference, detection of chromosomal DNA targets, and correction of genetic mutations.[1−7] Established approaches toward these ends entail the use of triplex-forming oligonucleotides (TFOs)[8] or peptide nucleic acids (PNAs),[9] minor-groove binding polyamides,[10,11] or engineered proteins such as zinc finger nucleases or transcription activator-like effector nucleases (TALENs).[3,12] While prominent advances have been made using these probe technologies, they do have limitations. For example, triplex-based approaches require the dsDNA targets to contain an extended purine-rich region, polyamides typically only recognize short target regions, and the construction of engineered proteins requires the use of nontrivial molecular cloning techniques. A range of alternative approaches addressing some of these limitations have been developed,[12−23] including pseudocomplementary PNA,[24−27] γ-PNA,[28,29] and the CRISPR/Cas (*c*lustered, *r*egularly *i*nterspaced, *s*hort *p*alindromic *r*epeat/CRISPR-*as*sociated protein) systems.[30] Nonetheless, there still is an unmet need for oligonucleotide-based probes that enable rapid, efficient, and site-specific mixed-sequence recognition of dsDNA target regions at physiological conditions.

We have been exploring a fundamentally different strategy toward this goal that entails the use of energetically activated DNA duplexes.[31−36] These so-called Invader probes are modified with +1 interstrand zippers arrangements of intercalator-functionalized nucleotides (Figure 1; see the Experimental Section for a definition of the zipper nomenclature). This particular structural motif forces the intercalators into the same region of the synthetic DNA duplex, leading to a violation of the "nearest neighbor exclusion principle",[37] according to which the highest intercalator density that will be accommodated in a DNA duplex is one intercalator for every two base pairs. As a result, duplexes with +1 interstrand zipper arrangements of intercalator-functionalized nucleotides are significantly perturbed and destabilized.[31−36] The two strands of the energetically activated duplex, on the other hand, display

Received: April 3, 2015
Published: May 18, 2015

DOI: 10.1021/acs.joc.5b00742
J. Org. Chem. 2015, 80, 5395−5406

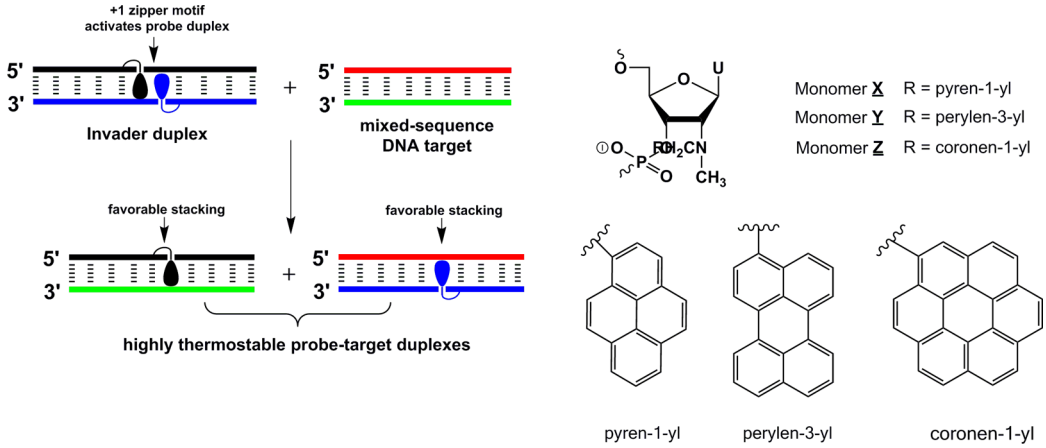

Figure 1. Illustration of the strategy for recognition of mixed-sequence dsDNA (shown with isosequential target) and monomer structures described herein. Droplets denote intercalating moieties.

very high affinity toward complementary DNA (cDNA) as duplex formation results in strongly stabilizing interactions between intercalators and neighboring base pairs (Figure 1). The energy difference between the Invader probe and the probe–target duplexes provides the driving force for recognition of dsDNA via dual duplex invasion.[31−36] Invader probes have been used for recognition of mixed-sequence dsDNA fragments specific to food pathogens[34] and for detection of gender-specific chromosomal DNA under non-denaturing conditions.[35]

First-generation Invader probes were based on 2′-*N*-(pyren-1-yl)-2′-amino-α-L-LNA (locked nucleic acid) monomers.[31] However, the challenging synthesis of these building blocks[38,39] prompted us to identify more readily available monomers. Two candidates emerged from these initial screens, i.e., 2′-*O*-(pyren-1-yl)methyl-RNA and 2′-*N*-(pyren-1-yl)-methyl-2′-*N*-methyl-2′-amino-DNA monomers (Figure 1).[32] Straightforward access to these building blocks[33,40] has enabled us to conduct structure–property relationship studies in which the influence of the nucleobase[33] and the orientation of the pyrene relative to the sugar skeleton[36] on dsDNA recognition has been delineated.

In the present study, we set out to study the impact of intercalator size on the dsDNA recognition efficiency of Invader probes. Until now, we have used pyrene-functionalized nucleotides as the key activating components of Invader probes. However, it is known that the surface area of pyrene (~220 Å^2) is smaller than the area occupied by natural base pairs (~270 Å^2).[41] The use of building blocks with larger intercalators therefore presents itself as a promising strategy for (i) additional destabilization of Invader probes (more pronounced violation of the "nearest neighbor exclusion principle"), (ii) increasing the cDNA affinity of individual Invader strands (more efficient intercalator-nucleobase stacking), and consequentially, (iii) increasing the thermodynamic driving force of Invader-mediated dsDNA recognition. Toward this end, we synthesized 2′-*N*-methyl-2′-amino-2′-deoxyuridine nucleotides that are N2′-functionalized with pyrene, perylene, or coronene moieties (Figure 1) and incorporated these building blocks into oligodeoxyribonucleotides (ONs). The resulting ONs and Invader probes are characterized by means of thermal denaturation experiments, analysis of thermodynamic parameters, absorption and fluorescence spectroscopy, and model dsDNA recognition experiments.

RESULTS AND DISCUSSION

Synthesis of N2′-Functionalized 2′-*N*-Methyl-2′-aminodeoxyuridine Phosphoramidites. Our original synthesis of phosphoramidite **4X** proceeded in only ~10% overall yield over seven steps from uridine, largely due to moderate yields during N2′-alkylation of 2′-amino-2′-deoxy-2′-*N*-methyl-5′-*O*-(4,4′-dimethoxytrityl)uridine (46% yield, $PyCH_2Cl/Et_3N$/THF/80 °C).[40] Reductive alkylation using 1-pyrenecarbaldehyde and sodium triacetoxyborohydride or sodium cyanoborohydride offered no improvement due to concomitant formation of cyclic N2′,O3′-hemiaminal ethers, which presumably are formed due to steric crowding at the 2′-position.[40]

Motivated by previous reports describing reductive alkylations on less hindered 2′-amino-2′-deoxyuridines,[42] we set out to devise a route to **4X** in which *N*-arylation is carried out prior to *N*-methylation and which can be adapted for the synthesis of **4Y** and **4Z**. O5′-DMTr protected 2′-amino-2′-deoxyuridine **1**, obtained in 65% yield from uridine over three steps,[43] was used as the starting material (Scheme 1). Reductive alkylation of **1** using sodium triacetoxyborohydride[44] and the appropriate aromatic aldehyde affords nucleosides **2X–2Z** (43–95%, Scheme 1). It is interesting to note that the reaction yield decreases with increasing bulk of the aromatic moiety. Subsequent reductive methylation using sodium triacetoxyborohydride and formaldehyde furnishes nucleosides **3X–3Z** in excellent yields. We found it necessary to use an excess of sodium triacetoxyborohydride to minimize formation of cyclic N2′,O3′-hemiaminal ethers during N2′-alkylations (Scheme 1). Treatment of nucleosides **3X–3Z** with 2-cyanoethyl *N*,*N*-diisopropylchorophosphoramidite (PCl reagent) and *N*,*N*-diisopropylethylamine affords target phosphoramidites **4X–4Z** in high yields. The new route to **4X** is a significant improvement over existing routes[40,42] (~52% yield from uridine over six steps versus 5–10% yield from uridine over seven or eight steps).

Synthesis of Modified ONs. Phosphoramidites **4X**, **4Y**, and **4Z** were used in machine-assisted solid-phase DNA synthesis to incorporate monomers **X–Z** into ONs using extended hand-coupling conditions (15 min) and the following activators: **4X** (5-[3,5-bis(trifluoromethyl)phenyl]-1*H*-tetrazole, ~99% coupling yield), **4Y** (pyridinium hydrochloride, ~90% coupling yield), and **4Z** (5-[3,5-bis(trifluoromethyl)-phenyl]-1*H*-tetrazole, ~80% coupling yield). Suitable activators

DOI: 10.1021/acs.joc.5b00742
J. Org. Chem. 2015, 80, 5395–5406

Scheme 1. Synthesis of N2′-Functionalized 2′-Amino-2′-deoxy-2′-*N*-methyluridine Phosphoramidites[a]

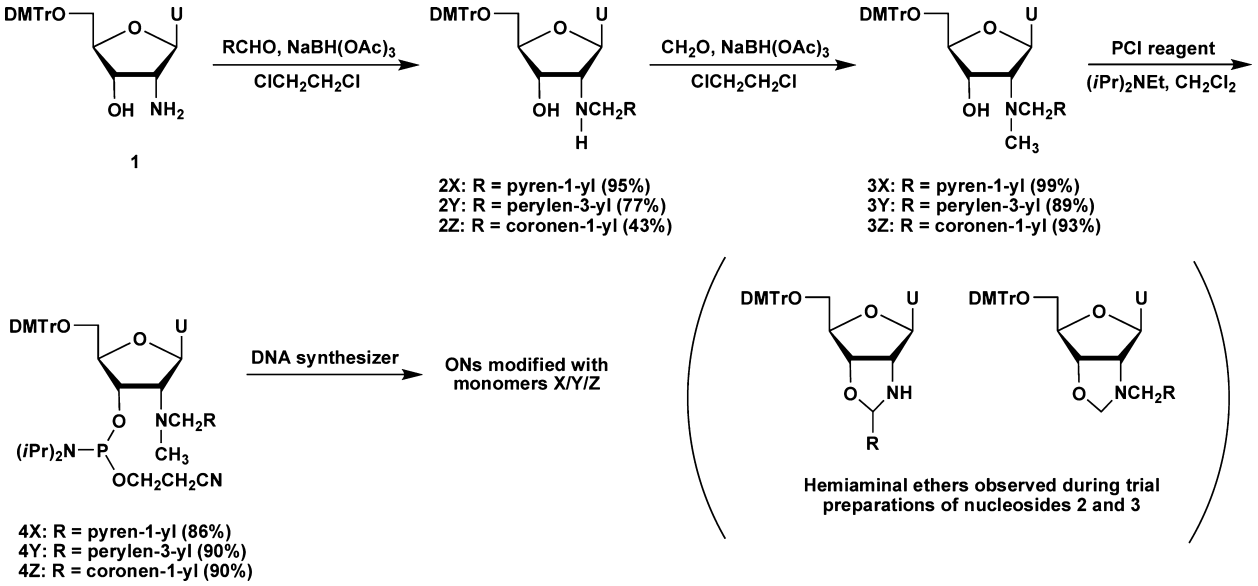

[a]U = uracil-1-yl; DMTr = 4,4′-dimethoxytrityl; PCl reagent = 2-cyanoethyl *N*,*N*-diisopropylchlorophosphoramidite.

Table 1. Thermal Denaturation Temperatures of Duplexes between B1−B6 and cDNA or cRNA Relative to Reference Duplexes[a]

			ΔT_m (°C)					
			+ cDNA			+ cRNA		
ON	sequence	B =	X	Y	Z	X	Y	Z
B1	5′-G**B**G ATA TGC		+5.0[b]	+11.5	+7.5	−2.0[b]	−6.5	+0.5
B2	5′-GTG A**B**A TGC		+15.0	+20.0	+21.0	+3.0	+7.0	+14.0
B3	5′-GTG ATA **B**GC		+9.0	+16.0	+14.0	−0.5	+2.5	+1.0
B4	3′-CAC **B**AT ACG		+1.5[b]	+11.5	+7.5	−6.5[b]	−4.0	+1.0
B5	3′-CAC TA**B** ACG		+15.0	+20.0	+20.0	+3.0[b]	+9.0	+11.0
B6	3′-CAC **B**A**B** ACG		+14.0[b]	+31.0	+24.5	−3.0[b]	+7.5	+7.0

[a]ΔT_m = change in T_m relative to reference duplexes **D1**:**D4** ($T_m \equiv 29.5$ °C), **D1**:**R4** ($T_m \equiv 27.5$ °C), or **R1**:**D4** ($T_m \equiv 27.5$ °C), where **D1**: 5′-GTG ATA TGC, **D4**: 3′-CAC TAT ACG, **R1**: 5′-GUG AUA UGC and **R4**: 3′-CAC UAU ACG; T_m's are determined as the maximum of the first derivative of melting curves (A_{260} vs T) recorded in medium salt phosphate buffer ($[Na^+]$ = 110 mM, $[Cl^-]$ = 100 mM, pH 7.0 (NaH_2PO_4/Na_2HPO_4)), using 1.0 μM of each strand. Reported T_m's are averages of at least two measurements within 1.0 °C; A = adenin-9-yl DNA monomer, C = cytosin-1-yl DNA monomer, G = guanin-9-yl DNA monomer, *T* = thymin-1-yl DNA monomer. For structures of monomers **X**−**Z**, see Figure 1. [b]Data previously reported in ref 40.

were identified through screening of common activators (results not shown). The identity and purity of the modified ONs was established through MALDI-TOF (Table S1, Supporting Information) and ion-pair reversed-phase HPLC (>85% purity), respectively. The perylene-modified ONs were found to be light sensitive and were therefore stored in the dark until use.

Monomers **Y** and **Z** were studied in the same 9-mer mixed sequence contexts that we have used for evaluation of other Invader building blocks.[32] Previously reported data for **X**-modified ONs is included to facilitate direct comparison. ONs containing a single incorporation in the 5′-GBG ATA TGC context are denoted **X1**, **Y1**, and **Z1**. Similar conventions apply for the **B2**−**B6** series (Table 1). Reference DNA and RNA strands are denoted **D1**/**D4** and **R1**/**R4**, respectively (see footnote a, Table 1).

Thermostability of Duplexes between Modified ONs and Complementary DNA/RNA. Thermal denaturation temperatures (T_m's) of duplexes between **B1**−**B6** and complementary DNA or RNA (cDNA/cRNA) were determined in medium salt phosphate buffer ($[Na^+]$ = 110 mM, pH 7.0). ONs with one incorporation of monomer **Y** or **Z** form exceptionally stable duplexes with cDNA (ΔT_m from +7.5 to +21.0 °C, Table 1). In fact, duplexes modified with perylene monomer **Y** are 5−10 °C more stable than the corresponding pyrene-modified duplexes (T_m trend: **Y** ≥ **Z** > **X**) and slightly more stable than duplexes modified with 2′-*N*-(pyren-1-yl)carbonyl-2′-amino-α-L-LNA-T monomers, which are among the most strongly stabilizing modified nucleotides reported until date.[32] Incorporation of a second monomer as a next-nearest neighbor results in near-additive increases in T_m's (compare ΔT_m's for **B4**-, **B5**-, and **B6**-series, Table 1). The degree of stabilization is strongly dependent on the sequence context, which is consistent with observations made with other intercalator-modified ONs.[33,45,46] For example, ONs in which the modification is flanked by 3′-purines form more stable duplexes than when flanked by 3′-pyrimidines (e.g., compare ΔT_m's for **B2** and **B4** series, Table 1). This suggests that the aromatic moieties intercalate in the 3′-direction, leading to particularly strong π−π-stacking interactions with purines.[46]

DOI: 10.1021/acs.joc.5b00742
J. Org. Chem. 2015, 80, 5395−5406

Table 2. Discrimination of Mismatched DNA Targets by X2/Y2/Z2 and Reference Strands[a]

			DNA: 3′-CAC TBT ACG			
			T_m (°C)	ΔT_m (°C)		
ON	sequence	B =	A	C	G	T
D1	5′-GTG ATA TGC		**29.5**	−16.5	−9.5	−17.0
X2[b]	5′-GTG AXA TGC		**44.5**	−23.0	−3.5	−13.0
Y2	5′-GTG AYA TGC		**49.5**	−19.5	−4.0	−17.0
Z2	5′-GTG AZA TGC		**50.5**	−15.5	−3.0	−15.5

[a]For experimental conditions, see Table 1. T_m's of fully matched duplexes are shown in bold. ΔT_m = change in T_m relative to fully matched duplex. [b]From ref 40.

Table 3. Discrimination of Mismatched DNA Targets by X6/Y6/Z6 and Reference Strands[a]

			DNA: 5′-GTG ABA TGC			
			T_m (°C)	ΔT_m (°C)		
ON	sequence	B =	T	A	C	G
D4	3′-CAC TAT ACG		**29.5**	−17.0	−15.5	−9.0
X6[b]	3′-CAC XAX ACG		**43.5**	−21.5	−10.5	−13.5
Y6	3′-CAC YAY ACG		**60.5**	−25.5	−22.5	−18.0
Z6	3′-CAC ZAZ ACG		**54.0**	−22.5	−16.5	−12.5

[a]For experimental conditions, see Table 1. T_m's of fully matched duplexes are shown in bold. ΔT_m = change in T_m relative to fully matched duplex. [b]From ref 40.

Table 4. Absorption Maxima in the 300-500 nm Region for X/Y/Z-Modified ONs and the Corresponding Duplexes with Complementary DNA or RNA[a]

			λ_{max} [$\Delta\lambda_{max}$] (nm)								
		B =	X[b]			Y			Z		
ON	sequence		SSP	+cDNA	+cRNA	SSP	+cDNA	+cRNA	SSP	+cDNA	+cRNA
B1	5′-GBG ATA TGC		349	353 [+4]	351 [+2]	448	450 [+2]	450 [+2]	312	314 [+2]	313 [+1]
B2	5′-GTG ABA TGC		348	353 [+5]	351 [+3]	451	453 [+2]	453 [+2]	313	314 [+1]	313 [±0]
B3	5′-GTG ATA BGC		349	353 [+4]	354 [+5]	451	452 [+1]	452 [+1]	313	314 [+1]	313 [±0]
B4	3′-CAC BAT ACG		349	354 [+5]	349 [±0]	450	452 [+2]	452 [+2]	312	314 [+2]	313 [+1]
B5	3′-CAC TAB ACG		348	354 [+6]	352 [+4]	450	450 [±0]	452 [+2]	313	314 [+1]	313 [±0]
B6	3′-CAC BAB ACG		ND	ND	ND	449	451 [+2]	452 [+3]	310	313 [+3]	313 [+3]

[a]Measurements were performed at 5 °C (**X**, **Y**) or 10 °C (**Z**) using a spectrophotometer and quartz optical cells with 1.0 cm path lengths. For buffer composition, see Table 1. ND = not determined. [b]Data for the **X** series, with the exception of **X3**, have been previously reported in ref 40.

Duplexes with cRNA are far less stable and, in some cases, even destabilized relative to reference duplexes (ΔT_m = −6.5 to +14.0 °C, Table 1; trend: **Z** > **Y** > **X**). This is another indicator of intercalative binding modes as intercalators generally favor the less compressed *B*-type helix geometry of DNA:DNA duplexes.[38−40,45,47−49] As a consequence, these ONs display significant selectivity for DNA targets, expressed as $\Delta\Delta T_m$ (DNA−RNA) = ΔT_m (vs cDNA) - ΔT_m (vs cRNA) > 0 °C, with **Y**-modified ONs displaying particularly remarkable DNA selectivity ($\Delta\Delta T_m$ (DNA−RNA) between 11.0 and 23.5 °C, Table S2).

Binding Specificity. The binding specificities of centrally modified ONs (**B2** series) were studied using DNA strands with mismatched nucleotides opposite to the modification (Table 2). **X2**/**Y2**/**Z2** discriminate C- and T-mismatched DNA targets with similar efficiency as unmodified **D1**, while G-mismatched DNA targets are poorly discriminated, indicating that the wobble base pair is greatly stabilized by the intercalating pyrene moiety.

ONs with two modifications positioned as next-nearest neighbors (**B6** series) display improved discrimination of DNA targets with a mismatched nucleotide opposite to the central 2′-deoxyadenosine residue, with binding specificity decreasing in the order: **Y6** > **Z6** ≥ **X6** (Table 3). DNA strands with mismatched A- and G-nucleotides are particularly efficiently discriminated. Similar specificity trends were observed for isosequential ONs modified with 2′-*O*-(pyren-1-yl)methyl-RNA.[36] For data with mismatched RNA targets, see Tables S3 and S4 in the Supporting Information.

These results indicate that **X**/**Y**/**Z**-modified ONs should be designed in a manner that places likely single nucleotide polymorphism (SNP) sites opposite to canonical 2′-deoxyribonucleotides rather than opposite to the modified monomers, if optimal discrimination of mismatched targets is to be ensured.

Photophysical Characterization of Modified ONs and Duplexes with Complementary DNA/RNA. UV−vis absorption and steady-state fluorescence emission spectra of **Y**- or **Z**-modified ONs were recorded in the absence or presence of cDNA/cRNA to gain further insight into the binding modes of the attached aromatic hydrocarbons. Hybridization of **Y**- or **Z**-modified ONs with cDNA/cRNA results in minor bathochromic shifts of the hydrocarbon absorption maxima ($\Delta\lambda_{max}$ = 0−3 nm, Table 4, Figures S2 and S3), which is indicative of ground-state electronic interactions between hydrocarbons and nucleobases and, hence, inter-

DOI: 10.1021/acs.joc.5b00742
J. Org. Chem. 2015, 80, 5395−5406

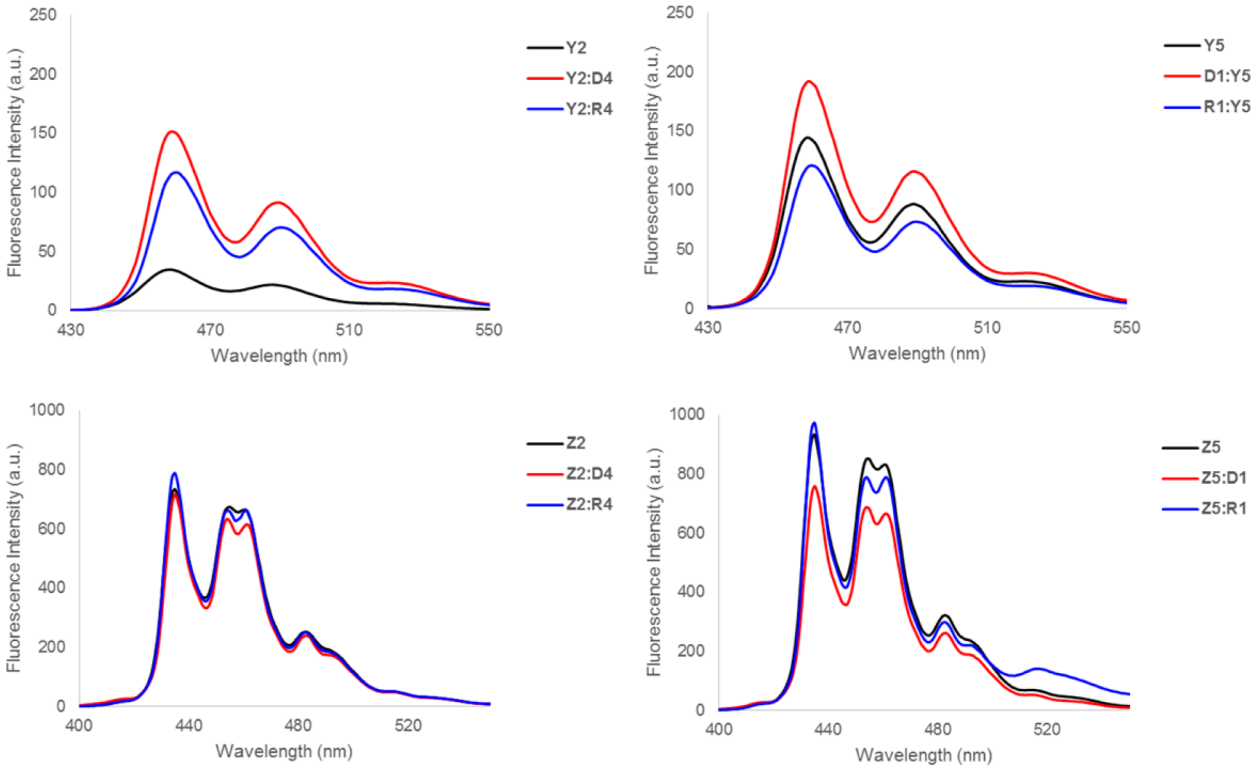

Figure 2. Steady-state fluorescence emission spectra of representative **Y**/**Z**-modified ONs and the corresponding duplexes with DNA/RNA targets. Spectra were recorded at 5 °C (**Y**-modified) or 10 °C (**Z**-modified) using λ_{ex} = 420 and 310 nm for **Y**- and **Z**-modified ONs, respectively. Each strand was used at 1.0 μM concentration in T_m buffer. Note: different axis scales are used.

calation.[50,51] However, the bathochromic shifts are smaller than for the pyrene-modified **X1**−**X6**. We speculate that this is because the perylene and coronene moieties are not fully contained within the duplex core.[52] Structural studies, beyond the scope of the present work, are necessary to verify this hypothesis.

Steady-state fluorescence emission spectra (λ_{ex} = 420 nm, T = 5 °C) of duplexes between perylene-modified **Y1**−**Y6** and cDNA/cRNA feature two bands at ∼460 nm and ∼490 nm (Figure 2 and Figure S4). Hybridization with DNA/RNA targets generally results in moderately increased fluorescence intensity (0.8- to 4.4-fold), with more pronounced increases being observed upon DNA binding. Similar trends have been noted with other perylene-functionalized ONs in which hybridization-induced intercalation is a likely binding mode. Unlike pyrene,[50,53−56] the fluorescence intensity of perylene is strongest in hydrophobic environments and much less sensitive to quenching by flanking nucleobases.[56−58]

Fluorescence emission spectra of coronene-modified **Z1**−**Z6** display three main emission peaks at ∼435, ∼455, and ∼483 nm along with several shoulders when excited at λ_{max} = 310 nm (T = 10 °C), which corresponds to a Stokes shift of >125 nm (Figure 2 and Figure S5). Hybridization with cDNA/cRNA has only a minor impact on fluorescence intensity, ranging from slight decreases (**Z5** vs cDNA) to moderate increases (**Z6** vs cDNA/cRNA). Although only few studies have been conducted with coronene-modified ONs,[59,60] it is interesting to note that isosequential ONs modified with closely related 2′-*O*-(coronen-1-yl)methyluridines display virtually identical photophysical characteristics,[60] which underscores intercalation as a likely binding mode.

Biophysical Properties of Duplexes with Interstrand Zippers of X/Y/Z Monomers. Having obtained evidence that the perylene and coronene moieties of **Y**- and **Z**-modified ONs intercalate upon duplex formation, a prerequisite for their potential use as Invader modifications, we went on to study double-stranded probes with different interstrand zipper arrangements of these monomers as potential dsDNA targeting probes (Table 5). The term thermal advantage (TA = ΔT_m (ON_A:cDNA) + ΔT_m (cDNA:ON_B) − ΔT_m (ON_A:ON_B), where ON_A:ON_B is a duplex with an interstrand zipper arrangement of monomers), serves as a first approximation to describe the energy difference between the "products" and "reactants" of the recognition process, with more positive values signifying greater dsDNA recognition potential.

Double-stranded probes with +1 monomer zippers hybridize more weakly and are more energetically activated for dsDNA recognition than probes with other zipper configurations (compare T_m's and TA values for **B2**:**B5** relative to other probe duplexes, Table 5), which mirrors the trends with other Invader probes.[31,32,35,36] According to this analysis, perylene-modified duplex **Y2**:**Y5** is the most strongly activated probe in this series. The coronene-modified **Z2**:**Z5** displays lower dsDNA targeting potential as the probe duplex is surprisingly stable (TA trend: **Y2**:**Y5** > **X2**:**X5** ≥ **Z2**:**Z5**, Table 5).

The above T_m-based conclusions are corroborated by thermodynamic parameters for duplex formation, which were derived via line fitting of denaturation curves.[61] Thus, formation of duplexes between **Y**- or **Z**-modified ONs and cDNA is considerably more favorable than formation of unmodified reference duplexes ($\Delta\Delta G^{293}$ between −24 and −6 kJ/mol, first and second ΔG^{293} columns, Table 5) and more favorable than the corresponding **X**-modified duplexes. The

DOI: 10.1021/acs.joc.5b00742
J. Org. Chem. 2015, 80, 5395−5406

Table 5. Biophysical Properties of X/Y/Z-Modified Probe Duplexes[a]

					$\Delta G^{293}[\Delta\Delta G^{293}]$ (kJ/mol)				
ON	ZP	probe duplex	T_m (°C)	TA (°C)	upper ON vs cDNA	lower ON vs cDNA	probe duplex	ΔG^{293}_{rec} (kJ/mol)	λ_{max} (nm)
X1 **X5**	**+4**	5′-G**X**G ATA TGC 3′-CAC TA**X** ACG	49.0	−1.5	−51 ± 1 [−6]	−64 ± 1 [−19]	N/A		353
X1 **X4**	**+2**	5′-G**X**G ATA TGC 3′-CAC **X**AT ACG	28.0	+8.0	−51 ± 1 [−6]	−48 ± 1 [−3]	−44 ± 1 [+1]	−10	350
X2 **X5**	**+1**	5′-GTG A**X**A TGC 3′-CAC TA**X** ACG	**28.5**	**+31.0**	**-65 ± 1 [−20]**	**−64 ± 1 [−19]**	**−44 ± 0 [+1]**	**−40**	**345**
X2 **X4**	**-1**	5′-GTG A**X**A TGC 3′-CAC **X**AT ACG	42.5	+2.5	−65 ± 1 [−20]	−48 ± 1 [−3]	−54 ± 1 [−9]	−14	352
Y1 **Y5**	**+4**	5′-G**Y**G ATA TGC 3′-CAC TA**Y** ACG	54.0	+8.5	−51 ± 0 [−6]	−69 ± 1 [−24]	−84 ± 3 [−39]	+9	452
Y1 **Y4**	**+2**	5′-G**Y**G ATA TGC 3′-CAC **Y**AT ACG	34.5	+18.0	−51 ± 0 [−6]	−58 ± 1 [−13]	−49 ± 0 [−4]	−15	450
Y2 **Y5**	**+1**	5′-GTG A**Y**A TGC 3′-CAC TA**Y** ACG	**32.5**	**+37.5**	**−69 ± 3 [−24]**	**−69 ± 1 [−24]**	**−49 ± 1 [−4]**	**-44**	**448**
Y2 **Y4**	**-1**	5′-GTG A**Y**A TGC 3′-CAC **Y**AT ACG	57.5	+1.0	−69 ± 3 [−24]	−58 ± 1 [−13]	−74 ± 4 [−29]	−8	452
Z1 **Z5**	**+4**	5′-G**Z**G ATA TGC 3′-CAC TA**Z** ACG	61.5	−4.5	−57 ± 0 [−12]	−66 ± 1 [−21]	−79 ± 1 [−34]	+1	314
Z1 **Z4**	**+2**	5′-G**Z**G ATA TGC 3′-CAC **Z**AT ACG	43.5	+1.5	−57 ± 0 [−12]	−57 ± 1 [−12]	−55 ± 1 [−10]	−14	313
Z2 **Z5**	**+1**	5′-GTG A**Z**A TGC 3′-CAC TA**Z** ACG	**41.0**	**+29.5**	**−68 ± 1 [−23]**	**−66 ± 1 [−22]**	**−54 ± 1 [−9]**	**−35**	**309**
Z2 **Z4**	**-1**	5′-GTG A**Z**A TGC 3′-CAC **Z**AT ACG	62.5	−4.5	−68 ± 1 [−23]	−57 ± 1 [−12]	−80 ± 1 [−35]	±0	314

[a]ZP = zipper. For conditions of thermal denaturation and absorption experiments, see Table 1 and Table 4, respectively. $TA_{ONA:ONB} = \Delta T_m$ (ON_A:cDNA) + ΔT_m(cDNA:ON_B) - ΔT_m (ON_A:ON_B). $\Delta\Delta G^{293}$ is measured relative to ΔG^{293} for **D1**:**D4** = −45 kJ/mol. ΔG^{293}_{rec} (**ON_A**:**ON_B**) = ΔG^{293} (**ON_A**:cDNA) + ΔG^{293} (cDNA:**ON_B**) − ΔG^{293} (**ON_A**:**ON_B**) − ΔG^{293} (dsDNA). "±" denotes standard deviation. N/A = the absence of a clear lower baseline precluded determination of this value. T_m's and TA's for all **X**-modified duplexes, except those involving **X3**, have been previously published in ref 32 but are included to facilitate direct comparison.

stabilization stems from favorably enthalpic contributions ($\Delta\Delta H$ < 0 kJ/mol in most cases, Table S5). Formation of **B2**:**B5** duplexes, as well as +2 zipper duplexes **B1**:**B4**, is 25−35 kJ/mol less favorable than duplexes with other interstrand zipper arrangements of **Y**- or **Z**-monomers (compare $\Delta\Delta G^{293}$ values in third ΔG^{293} column, Table 5). The energetic activation of the **B2**:**B5** probes is weakly enthalpic in nature ($\Delta\Delta H \geq 0$ kJ/mol for **B2**:**B5**, Table S5). Consequentially, **B2**:**B5** probes, and to a far lesser degree **B1**:**B4** probes, display favorable energetics for recognition of isosequential dsDNA targets as estimated by ΔG^{293}_{rec} (ON_A:ON_B) = ΔG^{293} (ON_A:cDNA) + ΔG^{293} (cDNA:ON_B) − ΔG^{293} (ON_A:ON_B) − ΔG^{293} (dsDNA) (i.e., $\Delta G^{293}_{rec} \ll 0$ kJ/mol, Table 5). The trend in the ΔG^{293}_{rec} values (**Y2**:**Y5** > **X2**:**X5** > **Z2**:**Z5**, Table 5) identifies the perylene-modified **Y2**:**Y5** as the most strongly activated probe for dsDNA recognition among the studied duplexes.

The results from the present and previous studies[31−36] clearly demonstrate that the activated nature is an inherent property of double-stranded probes with +1 interstrand zippers of monomers with intercalating moieties. Only this monomer configuration forces two intercalators into the same region within the duplex core, which leads to a violation of the "nearest-neighbor exclusion principle"[37] and structural perturbation of the duplex.[32,36] These structural effects also manifest themselves in the absorption maxima of the intercalators (Figure S6). Thus, significantly blue-shifted maxima are observed for **B2**:**B5** probes relative to probes with other zipper configurations (compare λ_{max} for **B2**:**B5** and other probe duplexes, Table 5), which indicates decreased interactions with neighboring nucleobases due to duplex perturbation. Moreover, **B2**:**B5** probes also exhibit distinct steady-state fluorescence emission spectra compared to probes with other zipper configurations (Figure 3). Thus, **X2**:**X5** displays the highest fluorescence intensity as intercalation-mediated duplex perturbation reduces pyrene-nucleobase interactions resulting in decreased fluorescence quenching. Conversely, **Y2**:**Y5** and **Z2**:**Z5** display low fluorescence intensity as intercalation-mediated duplex perturbation exposes the fluorophores to the polar and, in this case, quenching grooves. It is also interesting to point out that the emission spectrum of **Z2**:**Z5** contains less vibrational fine structure, which further indicates structural perturbation.

Recognition of DNA Hairpins Using Energetically Activated Probe Duplexes. The TA and ΔG^{293}_{rec} data identify probes with +1 interstrand zipper configurations of monomers **X**/**Y**/**Z** as the most thermodynamically activated constructs for dsDNA recognition. We therefore set out to experimentally test the recognition efficiency of these probes using a 3′-digoxigenin (DIG)-labeled DNA hairpin (DH), composed of a 9-mer double-stranded mixed sequence stem that is linked by a T_{10} loop, as a model dsDNA target (Figure 4a).[62] The feasibility of this target has been established in previous studies.[32,33,36] Incubation of **DH1** with **Y2**:**Y5**, **Z2**:**Z5**, or

DOI: 10.1021/acs.joc.5b00742
J. Org. Chem. 2015, 80, 5395−5406

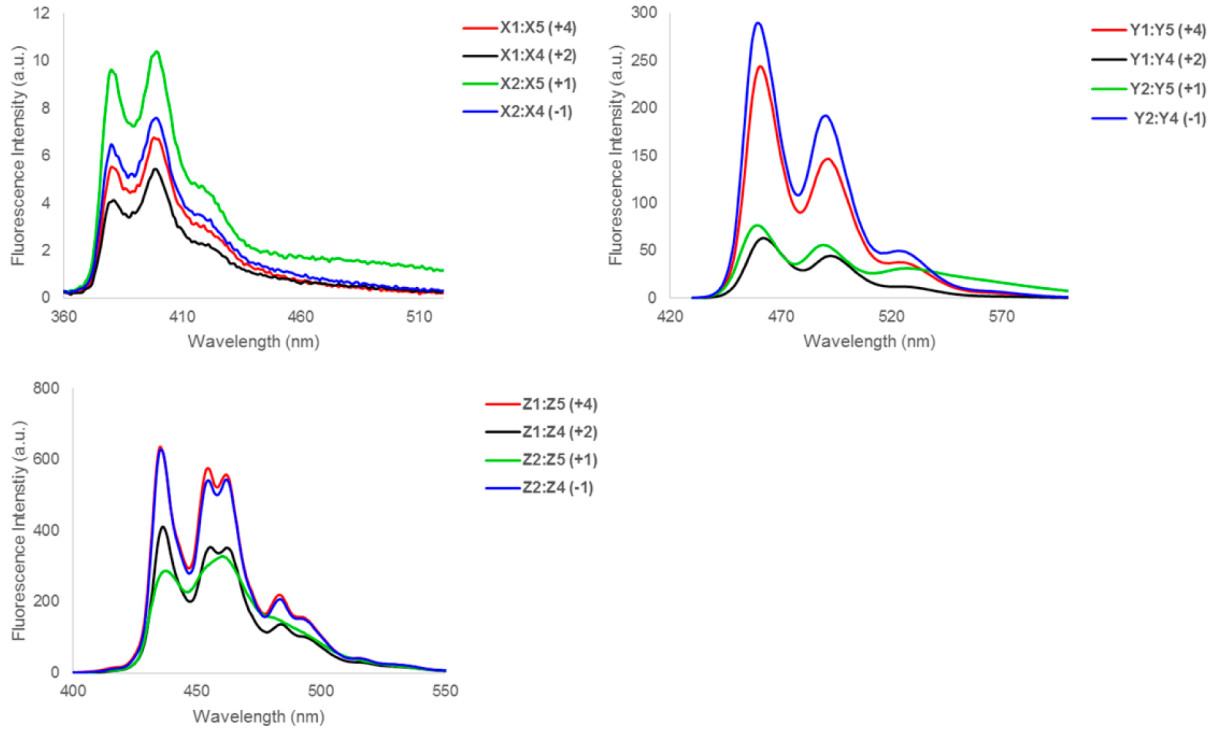

Figure 3. Steady-state fluorescence emission spectra of duplexes with different interstrand zippers of **X**, **Y**, or **Z** monomers (zipper type indicated in parentheses). For experimental conditions, see Figure 2. Spectra for **X**-modified duplexes, which were previously reported in ref 32, are included for comparison. Different axis scales are used.

benchmark Invader **X2**:**X5** in HEPES buffer at ambient temperature for 12−16 h results in dose-dependent formation of a more slowly migrating band in nondenaturing PAGE gels, which is indicative of ternary recognition complex formation (Figure 4c). Analysis of the corresponding dose−response curves reveals that **X2**:**X5**, **Y2**:**Y5**, and **Z2**:**Z5** display C_{50} values of ∼0.8, ∼0.5, and ∼0.6 μM, respectively (Figure 4d). It is particularly noteworthy that as little as 0.5 molar equiv of **Y2**:**Y5** or **Z2**:**Z5** results in ∼20% recognition of **DH1**. Complete recognition is accomplished when Invader probes are used at 100-fold molar excess relative to **DH1** (Figure 4d). Less recognition is observed when shorter incubation times (3 h) are used due to slow reaction kinetics (Figure S7). However, we have shown that recognition kinetics can be dramatically accelerated through incorporation of additional energetic hotspots.[31]

As a control, single-stranded ONs **X2**/**X5**/**Y2**/**Y5**/**Z2**/**Z5** were incubated with **DH1** for 12−16 h under otherwise identical conditions. Significantly less efficient dsDNA recognition is observed (C_{50} between 4.0 μM and >17.2 μM, Figures S8 and S9), underlining that both strands of an Invader probe are necessary to drive dsDNA recognition to completion.

Lastly, the binding specificities of **Y2**:**Y5**, **Z2**:**Z5**, and benchmark Invader **X2**:**X5** were studied by incubating the probes with DNA hairpins **DH2** and **DH3**, which are fully base-paired but which deviate in the nucleotide sequence at one or two positions relative to the Invader probes (underlined residues indicate sequence deviations, Figure 4b). Even when using **X2**:**X5**, **Y2**:**Y5**, or **Z2**:**Z5** at a 500-fold molar excess, mismatched DNA hairpins are not recognized, while complete recognition of matched **DH1** is observed (Figure 4e). This demonstrates that recognition of dsDNA using Invader probes based on N2′-pyrene-, perylene-, or coronene-functionalized 2′-*N*-methyl-2′-amino-DNA monomers proceeds both efficiently and with excellent specificity.

■ CONCLUSION

Efficient synthetic protocols for N2′-pyrene/perylene/coronene-functionalized 2′-*N*-methyl-2′-aminodeoxyuridine phosphoramidites have been developed. ONs that are modified with these building blocks form very stable duplexes with cDNA (ΔT_m/modification between +1.5 and +21.0 °C), with greater stabilization being observed with ONs modified with the large perylene and coronene moieties. The observed trends in absorption and fluorescence emission upon hybridization with cDNA, strongly suggests that the extraordinary duplex stabilization is due to intercalation of the labels. DNA duplexes with +1 interstrand zipper arrangements of these monomers are much less stable but their stability increases with intercalator size. The results from the present and previous studies[31−36] clearly demonstrate that the activated nature is an inherent property of double-stranded probes with +1 interstrand zippers of intercalator-functionalized monomers. As a consequence of these stability trends, Invader probes based on N2′-perylene-functionalized 2′-*N*-methyl-2′-amino-DNA monomers were predicted to be most strongly activated for dsDNA recognition. Experiments using DNA hairpins as model dsDNA targets confirmed this and, furthermore, showed that mixed-sequence recognition of dsDNA proceeds with excellent specificity. Invader probes based on N2′-intercalator-functionalized 2′-*N*-methyl-2′-amino-DNA monomers therefore present themselves as particularly interesting probes for dsDNA targeting applications in molecular biology, nucleic acid diagnostics, and biotechnology.

DOI: 10.1021/acs.joc.5b00742
J. Org. Chem. 2015, 80, 5395−5406

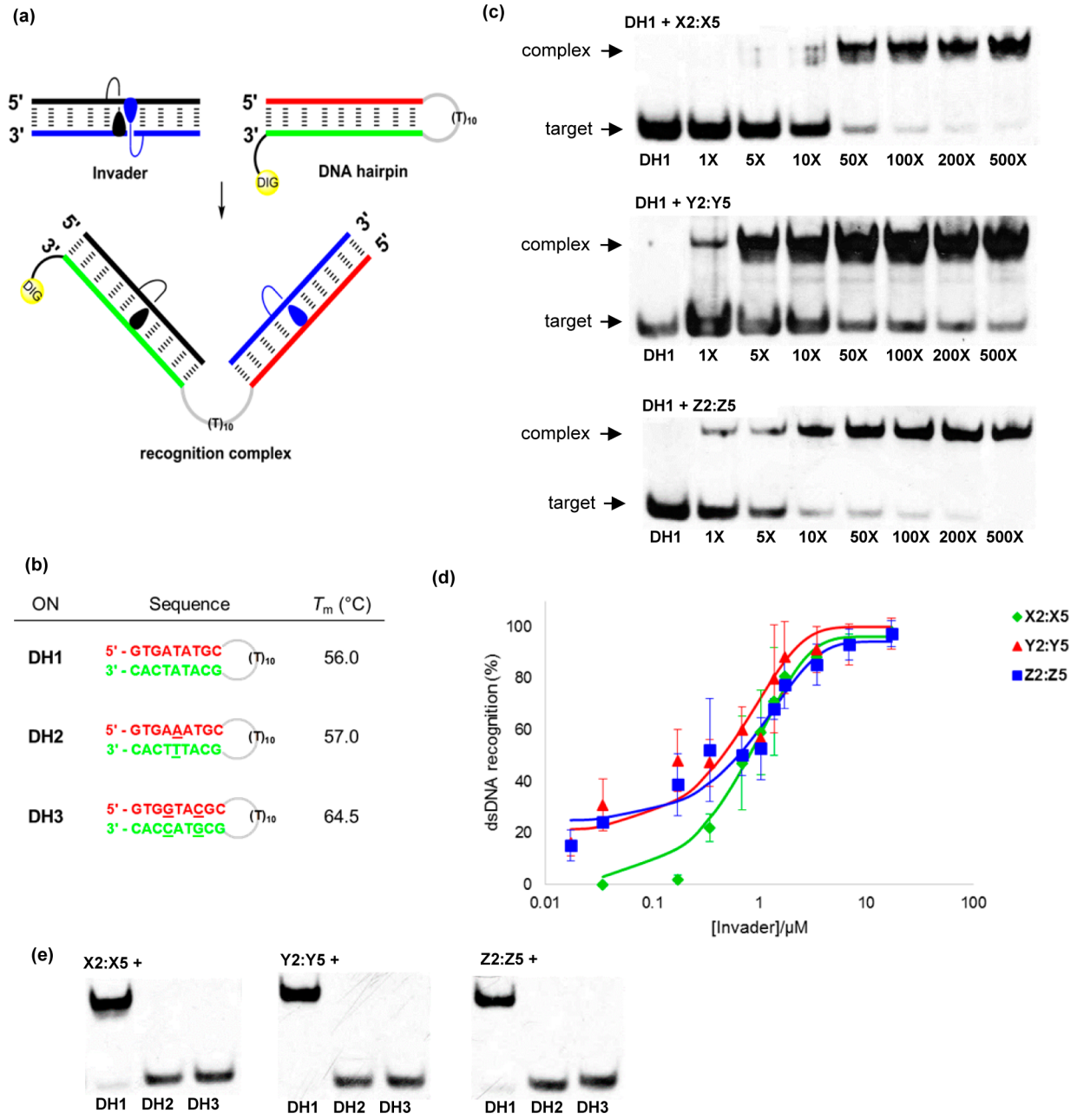

Figure 4. Recognition of DNA hairpins using activated double-stranded probes: (a) illustration of recognition process; (b) sequences of DNA hairpins with isosequential (**DH1**) or mismatched stems (**DH2** and **DH3**) (underlined nucleotides indicate positions of mismatches relative to probes); (c) representative electrophoretograms from recognition of **DH1** using 1- to 500-fold excess of **X2**:**X5**, **Y2**:**Y5**, or **Z2**:**Z5**; (d) dose–response curves (average of at least three independent experiments, error bars represent standard deviation); (e) electrophoretograms illustrating incubation of **DH1**–**DH3** with 500-fold molar excess of **X2**:**X5**, **Y2**:**Y5**, or **Z2**:**Z5**. Experimental conditions for electrophoretic mobility shift assay: separately preannealed targets (34.4 nM) and probes (variable concentrations) were incubated 12–16 h at ambient temperature in 1X HEPES buffer (50 mM HEPES, 100 mM NaCl, 5 mM $MgCl_2$, 10% sucrose, 1.4 mM spermine tetrahydrochloride, pH 7.2) and then run on 16% nondenaturing PAGE (performed at 70 V, 2.5 h, ~4 °C) using 0.5× TBE as a running buffer (45 mM Tris, 45 mM boric acid, 1 mM EDTA); DIG: digoxigenin.

EXPERIMENTAL SECTION

2′-Amino-2′-deoxy-2′-*N*-(pyren-1-ylmethyl)-5′-*O*-(4,4′-dimethoxytrityl)uridine (2X). Nucleoside **1** (200 mg, 0.37 mmol) was coevaporated with anhydrous 1,2-dichloroethane (2 × 3 mL) and redissolved in anhydrous 1,2-dichloroethane (2 mL). To this were added $NaBH(OAc)_3$ (120 mg, 0.55 mmol) and 1-pyrenecarboxaldehyde (105 mg, 0.44 mmol), and the reaction mixture was stirred under an argon atmosphere at room temperature for 5 h. Saturated aqueous $NaHCO_3$ (25 mL) was added, and the aqueous layer was extracted with CH_2Cl_2 (3 × 15 mL). The organic layers were dried (Na_2SO_4) and evaporated to dryness. The resulting residue was purified by silica gel column chromatography (0–4% MeOH in CH_2Cl_2, v/v) to afford **2X** (0.27 g, 95%) as a white foam: R_f = 0.5 (5% MeOH in CH_2Cl_2, v/v); MALDI-HRMS *m*/*z* 782.2849 ($[M + Na]^+$, $C_{47}H_{41}N_3O_7{\cdot}Na^+$, calcd 782.2837); ^{1}H NMR (500 MHz, DMSO-d_6) δ 11.37 (br s, ex, 1H, NH(U)), 8.45 (d, 1H, J = 9.1 Hz, Py), 8.26–8.29 (m, 2H, Py), 8.16–8.20 (m, 2H, Py), 8.14 (ap s, 2H, Py), 8.04–8.10 (m, 2H, Py), 7.60 (d, 1H, J = 8.2 Hz, H6), 7.28–7.32 (m, 2H, DMTr), 7.21–7.26 (m, 2H, DMTr), 7.15–7.20 (m, 5H, DMTr), 6.77–6.83 (m, 4H, DMTr), 5.92 (d, 1H, J = 6.3 Hz, H1′),

DOI: 10.1021/acs.joc.5b00742
J. Org. Chem. 2015, 80, 5395–5406

5.63 (d, ex, 1H, J = 5.8 Hz, 3′−OH), 5.19 (d, 1H, J = 8.2 Hz, H5), 4.49−4.59 (m, 2H, CH_2Py), 4.24−4.28 (m, 1H, H3′), 4.01−4.05 (m, 1H, H4′), 3.68 (s, 3H, CH_3O), 3.66 (s, 3H, CH_3O), 3.39−3.44 (m, 1H, H2′), 3.24−3.28 (dd, 1H, J = 10.6 Hz, 4.0 Hz, H5′), 3.16−3.20 (dd, 1H, J = 10.6 Hz, 3.3 Hz, H5′), 2.58−2.65 (m, ex, 1H, $NHCH_2$); ^{13}C NMR (125 MHz, DMSO-d_6) δ 162.8, 158.05, 158.02, 150.7, 144.4, 140.2 (C6), 135.3, 135.0, 134.1, 130.8, 130.3, 130.0, 129.7 (Ar), 129.6 (Ar), 128.5, 127.8 (Ar), 127.6 (Ar), 127.4 (Ar), 127.1 (Ar), 126.8 (Ar), 126.7 (Ar), 126.6 (Ar), 126.1 (Ar), 125.03 (Ar), 124.98 (Ar), 124.6 (Ar), 124.1, 124.0, 123.3 (Ar), 113.2 (Ar), 113.1 (Ar), 101.5 (C5), 87.3 (C1′), 85.9, 84.1 (C4′), 68.4 (C3′), 63.5 (C2′), 63.4 (C5′), 54.9 (OCH_3), 48.8 (CH_2Py).

2′-Amino-2′-deoxy-2′-*N*-(perylen-3-ylmethyl)-5′-*O*-(4,4′-dimethoxytrityl)uridine (2Y). Nucleoside **1** (0.28 g, 0.50 mmol) was coevaporated with anhydrous 1,2-dichloroethane (2 × 5 mL) and redissolved in anhydrous 1,2-dichloroethane (5 mL). To this was added $NaBH(OAc)_3$ (0.75 g, 3.53 mmol) followed by slow addition of 3-perylenecarboxaldehyde[63] (185 mg, 0.66 mmol) over 1.5 h. The reaction mixture was stirred under an argon atmosphere at room temperature for 22 h at which point it was diluted with EtOAc (30 mL) and washed with saturated aqueous $NaHCO_3$ (2 × 20 mL). The combined aqueous layers were back-extracted with EtOAc (3 × 15 mL), and the combined organic layers were dried (Na_2SO_4) and evaporated to dryness. The resulting residue was purified by silica gel column chromatography (0−100% EtOAc in petroleum ether, v/v) to afford **2Y** (0.32 g, 77%) as a yellow foam: R_f = 0.3 (5% MeOH in CH_2Cl_2, v/v); MALDI-HRMS m/z 832.3020 ($[M + Na]^+$, $C_{51}H_{43}N_3O_7{\cdot}Na^+$, calcd 832.2993); ^{1}H NMR (500 MHz, DMSO-d_6) δ 11.36 (br s, ex, 1H, NH(U)), 8.36 (t, 2H, J = 7.5 Hz, Pery), 8.29 (d, 1H, J = 7.5 Hz, Pery), 8.22 (d, 1H, J = 7.5 Hz, Pery), 8.03 (d, 1H, J = 8.5 Hz, Pery), 7.76−7.81 (m, 2H, Pery), 7.60−7.63 (d, 1H, J = 8.0 Hz, H6), 7.51−7.56 (m, 4H, Pery), 7.15−7.35 (m, 9H, DMTr), 6.81−6.86 (m, 4H, DMTr), 5.87 (d, 1H, J = 6.0 Hz, H1′), 5.63 (d, ex, 1H, J = 5.0 Hz, 3′−OH), 5.25 (d, 1H, J = 8.0 Hz, H5), 4.24−4.28 (m, 1H, H3′), 4.19−4.23 (m, 2H, CH_2Pery), 4.00−4.06 (m, 1H, H4′), 3.68 (s, 3H, CH_3O), 3.66 (s, 3H, CH_3O), 3.33−3.39 (m, 1H, H2′), 3.25−3.30 (m, 1H, H5′), 3.17−3.22 (m, 1H, H5′); ^{13}C NMR (125 MHz, DMSO-d_6) δ 162.8, 158.06, 158.03, 150.7, 144.4, 140.2 (C6), 135.9, 135.4, 135.1, 134.2, 132.6, 130.8, 130.6, 130.5, 129.7 (DMTr), 129.6 (DMTr), 128.2, 127.8 (Ar), 127.6 (Ar), 126.8 (Pery), 126.7 (Pery), 126.6 (Pery), 126.5 (Pery), 123.9 (Pery), 120.65 (Pery), 120.60 (Pery), 120.4 (Pery), 120.1 (Pery), 113.2 (DMTr), 113.1 (DMTr), 101.5 (C5), 87.2 (C1′), 85.9, 84.1 (C4′), 68.3 (C3′), 63.5 (C2′), 63.4 (C5′), 54.9 (CH_3O), 48.7 (CH_2Pery). A minor impurity of EtOAc was identified.[64]

2′-Amino-2′-deoxy-2′-*N*-(coronen-1-ylmethyl)-5′-*O*-(4,4′-dimethoxytrityl)uridine (2Z). Nucleoside **1** (0.30 g, 0.55 mmol) was coevaporated with anhydrous 1,2-dichloroethane (2 × 5 mL) and redissolved in anhydrous 1,2-dichloroethane (2.5 mL). This was slowly added over 1 h to a stirred solution of $NaBH(OAc)_3$ (240 mg, 1.10 mmol) and 1-coronenecarboxaldehyde[65] (0.27 g, 0.82 mmol) in anhydrous 1,2-dichloroethane (3 mL). The reaction mixture was stirred under an argon atmosphere at room temperature for 14 h at which point it was diluted with CH_2Cl_2 (40 mL) and washed with saturated aqueous $NaHCO_3$ (2 × 20 mL) and H_2O (20 mL). The organic layer was dried (Na_2SO_4) and evaporated to dryness. The resulting residue was purified by silica gel column chromatography (0−1.5% MeOH in CH_2Cl_2, v/v, initially built with 0.5% Et_3N) to afford **2Z** (205 mg, 43%) as a pale yellow foam: R_f = 0.8 (10% MeOH in CH_2Cl_2, v/v); MALDI-HRMS m/z 880.2998 ($[M + Na]^+$, $C_{55}H_{43}N_3O_7{\cdot}Na^+$, calcd 880.2993); ^{1}H NMR (500 MHz, DMSO-d_6) δ 11.45 (br s, ex, 1H, NH(U)), 9.16−9.18 (d, 1H, J = 9.0 Hz, Cor), 8.91−9.00 (m, 7H, Cor), 8.90 (d, 1H, J = 1.7 Hz, Cor), 8.88 (s, 1H, Cor), 8.74−8.76 (d, 1H, J = 8.5 Hz, Cor), 7.63 (d, 1H, J = 8.2 Hz, H6), 7.04−7.27 (m, 9H, DMTr), 6.69 (d, 2H, J = 9.0 Hz, DMTr), 6.65 (d, 2H, J = 9.0 Hz, DMTr), 6.07 (d, 1H, J = 6.5 Hz, H1′), 5.74 (d, ex, 1H, J = 4.4 Hz, 3′−OH − overlap with residual CH_2Cl_2), 5.14 (d, 1H, J = 8.2 Hz, H5), 4.98 (dd, 2H, J = 13.7 Hz, 4.1 Hz, CH_2Cor), 4.33−4.39 (m, 1H, H3′), 4.09−4.12 (m, 1H, H4′), 3.60−3.63 (m, 1H, H2′), 3.53 (s, 3H, CH_3O), 3.47 (s, 3H, CH_3O), 3.25−3.30 (dd, 1H, J = 10.5 Hz, 4.2 Hz, H5′), 3.18−3.22 (dd, 1H, J = 10.5 Hz, 3.5 Hz, H5′), 2.91−2.97 (m, ex, 1H, NH); ^{13}C NMR (125 MHz, DMSO-d_6) δ 162.9, 157.95, 157.89, 150.8, 144.3, 140.2 (C6), 135.3, 135.0, 134.7, 129.6 (DMTr), 129.5 (DMTr), 128.24, 128.15, 128.04, 127.97, 127.73, 127.70 (DMTr), 127.6 (DMTr), 126.9, 126.6 (DMTr), 126.3 (Cor), 126.24, 126.23 (Cor), 126.21 (Cor), 126.1 (Cor), 126.0 (Cor), 125.2 (Cor), 122.4 (Cor), 122.0, 121.7, 121.6, 121.4, 121.3, 120.9, 113.05 (DMTr), 113.01 (DMTr), 101.5 (C5), 87.3 (C1′), 85.9, 84.3 (C4′), 68.5 (C3′), 63.7 (C2′), 63.5 (C5′), 54.8 (CH_3O), 54.7 (CH_3O), 49.5 (CH_2Cor).

General Procedure for Preparation of Nucleosides 3 (Description for ∼1 mmol Scale). The appropriate nucleoside **2** was dissolved in anhydrous 1,2-dichloroethane. To this was added $NaBH(OAc)_3$ followed by dropwise addition of 37% aqueous solution of CH_2O (stabilized with ∼12% MeOH) over 30 s. The reaction mixture was then stirred under an argon atmosphere at room temperature until analytical TLC indicated completion (quantities and reaction times are specified below). The reaction mixture was then worked up and purified as specified below to afford nucleosides **3** (yields specified below).

2′-Amino-2′-deoxy-2′-N-methyl-2′-N-(pyren-1-ylmethyl)-5′-O-(4,4′-dimethoxytrityl)uridine (3X). Nucleoside **2X** (1.30 g, 1.71 mmol), $NaBH(OAc)_3$ (3.63 g, 17.1 mmol), CH_2O (37% solution, 130 μL, 2.57 mmol), and anhydrous 1,2-dichloroethane (12 mL) were reacted as described above (4 h). Saturated aqueous $NaHCO_3$ (100 mL) was added very slowly, and the aqueous layer was extracted with CH_2Cl_2 (2 × 50 mL). The combined organic layers were dried (Na_2SO_4) and evaporated to dryness, and the resulting residue was purified by silica gel column chromatography (0−5% MeOH in CH_2Cl_2, v/v) to afford **3X** (1.35 g, quant) as a white foam: R_f = 0.4 (5% MeOH in CH_2Cl_2, v/v); MALDI-HRMS m/z 796.2969 ($[M + Na]^+$, $C_{48}H_{43}N_3O_7{\cdot}Na^+$, calcd 796.2993); ^{13}C NMR is in agreement with previous data.[40]

2′-Amino-2′-deoxy-2′-*N*-methyl-2′-*N*-(perylen-3-ylmethyl)-5′-*O*-(4,4′-dimethoxytrityl)uridine (3Y). Nucleoside **2Y** (1.00 g, 1.23 mmol), $NaBH(OAc)_3$ (2.61 g, 12.3 mmol), CH_2O (37% solution, 100 μL, 1.86 mmol), and anhydrous 1,2-dichloroethane (20 mL) were reacted as described above (7 h). The reaction mixture was diluted with EtOAc (100 mL) and very slowly washed with saturated aqueous $NaHCO_3$ (2 × 75 mL). The combined aqueous layer was back-extracted with EtOAc (3 × 30 mL), and the combined organic layers were dried (Na_2SO_4) and evaporated to dryness. The resulting residue was purified by silica gel column chromatography (0−60% EtOAc in petroleum ether, v/v) to afford **3Y** (0.91 g, 89%) as a bright yellow foam: R_f = 0.4 (60% EtOAc in petroleum ether, v/v); MALDI-HRMS m/z 846.3174 ($[M + Na]^+$, $C_{52}H_{45}N_3O_7{\cdot}Na^+$, calcd 846.3150); ^{1}H NMR (500 MHz, DMSO-d_6) δ 11.39 (br d, ex, J = 2.0 Hz, NH(U)), 8.33−8.37 (m, 2H, Pery), 8.29 (d, 1H, J = 8.0 Hz, Pery), 8.23 (d, 1H, J = 8.0 Hz, Pery), 8.08 (d, 1H, J = 8.0 Hz, Pery), 7.76−7.80 (m, 2H, Pery), 7.60 (d, 1H, J = 8.0 Hz, H6), 7.42−7.55 (m, 4H, Pery), 7.18−7.40 (m, 9H, DMTr), 6.83−6.91 (m, 4H, DMTr), 6.39 (d, 1H, J = 8.5 Hz, H1′), 5.48 (d, ex, 1H, J = 5.5 Hz, 3′−OH), 5.43 (dd, 1H, J = 8.0 Hz, 2.0 Hz, H5), 4.37−4.41 (m, 1H, H3′), 4.10−4.18 (2d, 2H, J = 13.3 Hz, CH_2−pery), 4.02−4.06 (m, 1H, H4′), 3.71 (s, 3H, CH_3O), 3.70 (s, 3H, CH_3O), 3.35−3.41 (m, 1H, H2′), 3.27−3.31 (m, 1H, H5′ - partial overlap with H_2O signal), 3.15−3.19 (m, 1H, H5′), 2.37 (s, 3H, CH_3); ^{13}CNMR (125 MHz, DMSO-d_6) δ 162.7, 158.09, 158.08, 150.5, 144.5, 140.1 (C6), 135.4, 135.1, 134.5, 134.2, 133.0, 130.64, 130.58, 130.4, 130.0, 129.73 (DMTr), 129.67 (DMTr), 129.6, 128.3, 128.1 (Pery), 127.83 (DMTr), 127.78 (DMTr), 127.72 (Pery), 127.65 (DMTr), 127.62, 126.84 (Pery), 126.80 (Pery), 126.7 (DMTr), 126.3 (Pery), 124.7 (Pery), 120.6 (Pery), 120.4 (Pery), 120.0 (Pery), 113.21 (DMTr), 113.19 (DMTr), 102.0 (C5), 85.9, 85.1 (C4′), 83.2 (C1′), 71.2 (C3′), 67.6 (C2′), 64.1 (C5′), 57.7 (CH_2Pery), 55.0 (CH_3O), 38.6 (NCH_3 − overlap with DMSO-d_6 signal).

2′-Amino-2′-deoxy-2′-N-methyl-2′-N-(coronen-1-ylmethyl)-5′-O-(4,4′-dimethoxytrityl)uridine (3Z). Nucleoside **2Z** (120 mg, 0.14 mmol), $NaBH(OAc)_3$ (0.39 g, 1.40 mmol), CH_2O (37% solution, 12 μL, 0.21 mmol), and anhydrous 1,2-dichloroethane (2 mL) were

DOI: 10.1021/acs.joc.5b00742
J. Org. Chem. 2015, 80, 5395−5406

reacted as described above (5 h). The reaction mixture was diluted with CH_2Cl_2 (20 mL) and very slowly washed with saturated aqueous $NaHCO_3$ (2 × 20 mL). The aqueous was back-extracted with CH_2Cl_2 (2 × 10 mL) and the combined organic layers were dried (Na_2SO_4) and evaporated to dryness. The resulting residue was purified by silica gel column chromatography (0−2% MeOH in CH_2Cl_2, v/v initially built with 0.5% Et_3N, v/v) to afford **3Z** (113 mg, 93%) as a pale yellow foam: R_f = 0.7 (5% MeOH in CH_2Cl_2, v/v); MALDI-HRMS m/z 894.3161 ($[M + Na]^+$, $C_{56}H_{45}N_3O_7{\cdot}Na^+$, calcd 894.3155); ^{1}H NMR (500 MHz, $CDCl_3$) δ 9.10 (br s, 1H, ex, NH(U)), 8.91−8.95 (d, 1H, J = 8.8 Hz, Cor), 8.70 (d, 1H, J = 8.8 Hz, Cor), 8.50−8.67 (m, 7H, Cor), 8.46 (br s, 1H, Cor), 8.39−8.42 (d, 1H, J = 8.5 Hz, Cor), 7.91 (d, 1H, J = 8.0 Hz, H6), 7.30−7.35 (m, 2H, DMTr), 7.16−7.27 (m, 7H, DMTr−partial overlap with $CDCl_3$), 6.71−6.78 (m, 5H, DMTr + H1′), 5.34 (d, 1H, J = 8.0 Hz, H5), 4.93 (d, 1H, J = 12.5 Hz, CH_2Cor), 4.45 (d, 1H, J = 12.5 Hz, CH_2Cor), 4.17−4.22 (m, 1H, H3′), 4.12−4.15 (m, 1H, H4′), 3.98 (br s, 1H, ex, 3′−OH), 3.71 (s, 3H, CH_3O), 3.69 (s, 3H, CH_3O), 3.58−3.62 (m, 1H, H2′), 3.41−3.45 (dd, 1H, J = 10.5 Hz, 2.8 Hz, H5′), 3.33−3.37 (dd, 1H, J = 10.5 Hz, 2.8 Hz, H5′), 2.54 (s, 3H, NCH_3); ^{13}CNMR (125 MHz, $CDCl_3$) δ 163.2, 158.98, 158.95, 150.6, 144.5, 140.7 (C6), 135.4, 135.2, 131.1, 130.4 (DMTr), 130.3 (DMTr), 128.8, 128.6, 128.54, 128.50, 128.4 (Ar), 128.2 (Ar), 128.1 (Ar), 127.7, 127.4 (DMTr), 127.3, 126.5 (Cor), 126.4 (Cor), 126.3 (Cor), 126.2 (Cor), 126.1 (Cor), 126.0 (Cor), 125.8 (Cor), 123.0, 122.5, 122.3, 122.2, 122.0 (Cor), 113.5 (DMTr), 103.3 (C5), 87.5, 85.4 (C4′), 84.9 (C1′), 70.7 (C2′), 70.5 (C3′), 63.7 (C5′), 60.2 (CH_2Cor), 55.4 (CH_3O), 40.5 (NCH_3).

General Procedure for Preparation of Nucleosides 4 (Description for ∼1 mmol Scale). The appropriate nucleoside **3** was coevaporated with anhydrous 1,2-dichloroethane (10 mL) and redissolved in anhydrous CH_2Cl_2. To this was added anhydrous *N*,*N*-diisopropylethylamine (DIPEA) followed by dropwise addition of 2-cyanoethyl *N*,*N*-diisopropylchlorophosphoramidite (PCl reagent) and the reaction mixture was allowed to stir under an argon atmosphere at room temperature until analytical TLC indicated complete conversion (quantities and reaction times are specified below). Unless otherwise mentioned, cold EtOH (1 mL) was added and all solvents were evaporated off. The resulting residue was purified by silica gel column chromatography and subsequent precipitation from CH_2Cl_2 and petroleum ether to afford the desired phosphoramidite **4**.

*2′-Amino-2′-deoxy-2′-N-methyl-2′-N-(pyren-1-yl-methyl)-3′-O-(N,N-diisopropylamino-2-cyanoethoxyphosphinyl)-5′-O-(4,4′-dimethoxytrityl)uridine (**4X**).* Nucleoside **3X** (1.34 g, 1.73 mmol), PCl reagent (0.77 mL, 3.46 mmol), anhydrous DIPEA (1.50 mL, 8.67 mmol), and anhydrous CH_2Cl_2 (20 mL) were reacted and worked up as described above (2.5 h). Purification by silica gel column chromatography (0−50% EtOAc in petroleum ether, v/v) and precipitation from CH_2Cl_2 and petroleum ether afforded nucleoside **4X** as a white foam (1.45 g, 86%): R_f = 0.5 (50% EtOAc in petroleum ether, v/v); MALDI-HRMS m/z 996.4083 ($[M + Na]^+$, $C_{57}H_{60}N_5O_8P{\cdot}Na^+$, calcd 996.4077); ^{31}P NMR (121 MHz, $CDCl_3$) δ 151.0, 149.8. ^{31}P NMR data are in agreement with literature data.[40,42]

*2′-Amino-2′-deoxy-2′-N-methyl-2′-N-(perylen-3-ylmethyl)-3′-O-(N,N-diisopropylamino-2-cyanoethoxyphosphinyl)-5′-O-(4,4′-dimethoxytrityl)uridine (**4Y**).* Nucleoside **3Y** (0.40 g, 0.49 mmol), PCl reagent (220 μL, 0.97 mmol), anhydrous DIPEA (0.34 mL, 1.94 mmol), and anhydrous CH_2Cl_2 (5 mL) were reacted as described above (2 h). Absolute EtOH (∼1 mL) was added, and the reaction mixture was diluted with CH_2Cl_2 (30 mL) and washed with saturated aqueous $NaHCO_3$ (20 mL). The aqueous layer was back-extracted with CH_2Cl_2 (2 × 10 mL), and the combined organic layer was dried (Na_2SO_4) and evaporated to dryness. The resulting residue was purified by silica gel column chromatography (0−50% EtOAc in petroleum ether, v/v) to afford nucleoside **4Y** (0.45 g, 90%) as a bright yellow foam: R_f = 0.4 (60% EtOAc in petroleum ether, v/v); MALDI-HRMS m/z 1046.4272 ($[M + Na]^+$, $C_{61}H_{62}N_5O_8P{\cdot}Na^+$, calcd 1046.4228); ^{31}P NMR (121 MHz, $CDCl_3$) δ 150.9, 149.7.

*2′-Amino-2′-deoxy-2′-N-methyl-2′-N-(coronen-1-ylmethyl)-3′-O-(N,N-diisopropylamino-2-cyanoethoxyphosphinyl)-5′-O-(4,4′-dimethoxytrityl)uridine (**4Z**).* Nucleoside **3Z** (0.27 g, 0.31 mmol), PCl reagent (210 μL, 0.93 mmol), anhydrous DIPEA (0.27 mL, 1.55 mmol), and anhydrous CH_3CN (1.5 mL) were reacted and worked up as described above (2.5 h). Purification by silica gel column chromatography (0−1% MeOH in CH_2Cl_2, v/v, initially built with 0.5% Et_3N, v/v) and precipitation from CH_2Cl_2 and petroleum ether afforded nucleoside **4Z** (0.30 g, 90%) as a pale yellow foam: R_f = 0.6 (3% MeOH in CH_2Cl_2, v/v); MALDI-HRMS m/z 1072.4399 ($[M + H]^+$, $C_{65}H_{62}N_5O_8P{\cdot}H^+$, calcd 1072.4409); ^{31}P NMR (121 MHz, $CDCl_3$) δ 151.0, 149.8.

Protocol: Synthesis and Purification of ONs. Modified ONs were synthesized on a 0.2 μmol scale using a DNA synthesizer and succinyl linked LCAA-CPG (long chain alkyl amine controlled pore glass) columns with a pore size of 500 Å. Standard protocols for incorporation of DNA monomers were used. The following hand-coupling conditions were used for incorporation of monomers **X**-**Z** (coupling time; activator; coupling yield): **4X** (15 min; 5-[3,5-bis(trifluoromethyl)phenyl]-1*H*-tetrazole; ∼99%), **4Y** (15 min; pyridinium hydrochloride; ∼90%) and **4Z** (15 min; 5-[3,5-bis-(trifluoromethyl)phenyl]-1*H*-tetrazole; CH_2Cl_2; ∼80%). All modified phosphoramidites were used at 50-fold molar excess and 0.05 M concentration in CH_3CN (**4X**) or CH_2Cl_2 (**4Y**/**4Z**). Extended oxidation (45 s) was used. Cleavage from solid support and removal of protecting groups was accomplished upon treatment with 32% aq ammonia (55 °C, 12 h). ONs were purified in the DMT-on mode via ion-pair reversed-phase HPLC (C18 column) using a 0.05 M triethylammonium acetate−water/acetonitrile gradient. This was followed by detritylation (80% aq AcOH) and precipitation ($NaOAc/NaClO_4$/acetone, −18 °C for 12−16 h). The identity of synthesized ONs was established through MALDI-MS analysis (Table S1) recorded in positive-ion mode on a quadrupole time-of-flight tandem mass spectrometer equipped with a MALDI source using anthranilic acid, 3-hydroxypicolinic acid (3-HPA), or 2′,4′,6′-trihydroxyacetophenone (THAP) as matricies. Purity was verified by ion-pair reversed-phase HPLC running in analytical mode (>85%). ONs modified with monomer **Y** were stored in the dark (wrapped in aluminum foil) to prevent light-induced bleaching/degradation of the fluorophore. ONs stored in this manner were stable for at least 12 months (>85% purity).

Protocol: Thermal Denaturation Studies. ON concentrations were estimated using the following extinction coefficients for DNA (OD/μmol): G (12.01), A (15.20), T (8.40), C (7.05); RNA (OD/μmol): G (13.70), A (15.40), U (10.00), C (9.00); and hydrocarbons (OD/μmol): pyrene (22.4),[66] perylene (33.2),[67] and coronene (36.0).[59] Strands were thoroughly mixed and denatured by heating to 70−85 °C, followed by cooling to the starting temperature of the experiment. Quartz optical cells with a path length of 1.0 cm were used. Thermal denaturation temperatures (T_m's) of duplexes (1.0 μM final concentration of each strand) were measured using a UV/vis spectrophotometer equipped with a 12-cell Peltier temperature controller and determined as the maximum of the first derivative of the thermal denaturation curve (A_{260} vs T) recorded in medium salt phosphate buffer (T_m buffer: 100 mM NaCl, 0.1 mM EDTA and pH 7.0 adjusted with 10 mM Na_2HPO_4 and 5 mM Na_2HPO_4). The temperature of the denaturation experiments ranged from at least 15 °C below T_m to 20 °C above T_m (although not below 3 °C). A temperature ramp of 0.5 °C/min was used in all experiments. Reported T_m's are averages of two experiments within ±1.0 °C.

Protocol: Determination of Thermodynamic Parameters. Thermodynamic parameters for duplex formation were determined through baseline fitting of denaturation curves (van't Hoff analysis) using software provided with the UV/vis spectrometer. Bimolecular reactions, two-state melting behavior, and a heat capacity change of ΔC_p = 0 upon hybridization were assumed.[61] A minimum of two experimental denaturation curves were each analyzed at least three times to minimize errors arising from baseline choice. Averages and standard deviations are listed.

DOI: 10.1021/acs.joc.5b00742
J. Org. Chem. 2015, 80, 5395−5406

Protocol: Absorption Spectra. UV−vis absorption spectra (range 200−600 nm) were recorded at 5 °C (**X**- and **Y**-modified ONs/duplexes) or 10 °C (**Z**-modified ONs/duplexes) using the same samples and instrumentation as in the thermal denaturation experiments.

Protocol: Steady-State Fluorescence Emission Spectra. Steady-state fluorescence emission spectra of ONs modified with monomers **X**-**Z** and the corresponding duplexes with complementary DNA/RNA targets, were recorded in nondeoxygenated thermal denaturation buffer (each strand at 1.0 μM concentration) and obtained as an average of five scans using an excitation wavelength of λ_{ex} = 350, 420, or 310 nm for **X**-, **Y**-, or **Z**-modified ONs, respectively. Excitation and emission slits of 5.0 and 2.5 nm, respectively were used along with a scan speed of 600 nm/min. Experiments were determined at 5 °C (**X**/**Y**) or 10 °C (**Z**) under N_2 flow to ascertain maximal hybridization of probes to DNA/RNA targets.

Protocol: Electrophoretic Mobility Shift Assay. This assay was performed essentially as previously described.[35] Unmodified DNA hairpins **DH1**−**DH3** were obtained from commercial sources and used without further purification. The DNA hairpins were 3′-DIG-labeled using the second-generation DIG Gel Shift Kit (Roche Applied Bioscience) per the manufacturer's recommendation. DIG-labeled ONs obtained in this manner were diluted and used without further purification in the recognition experiments. Preannealed probes (85 °C for 10 min, cooled to room temperature over 15 min) and DIG-labeled DNA hairpins (34.4 nM) were mixed and incubated in HEPES buffer (50 mM HEPES, 100 mM NaCl, 5 mM $MgCl_2$, 10% sucrose, 1.44 mM spermine tetrahydrochloride, pH 7.2) for the specified time at ambient temperature (~21 ± 3 °C). The reaction mixtures were then diluted with 6x DNA loading dye (Fermentas) and loaded onto a 16% nondenaturing polyacrylamide gel. Electrophoresis was performed using a constant voltage of 70 V for 2.5 h at ~4 °C using 0.5x TBE as a running buffer (45 mM Tris, 45 mM boric acid, 1 mM EDTA). Gels were blotted onto positively charged nylon membranes (Roche Applied Bioscience) using constant voltage with external cooling (100 V, ~4 °C). The membranes were exposed to antidigoxigenin-AP F_{ab} fragments as recommended by the manufacturer of the DIG Gel Shift Kit, transferred to a hybridization jacket, and incubated with the substrate (CSPD) in detection buffer for 10 min at 37 °C. The chemiluminescence of the formed product was captured on X-ray film, which was developed using an X-Omatic 1000A X-ray film developer (Kodak). The resulting bands were quantified using ImageJ software. Invasion efficiency was determined as the intensity ratio between the recognition complex band and the total lane. An average of three independent experiments is reported along with standard deviations. Nonlinear regression was used to fit data points from dose−response experiments, using a script written for the "Solver" module in Microsoft Office Excel.

Explanation of Zipper Nomenclature. The following nomenclature describes the relative arrangement between two monomers positioned on opposing strands in a duplex. The number *n* describes the distance measured in number of base pairs and has a positive value if a monomer is shifted toward the 5′-side of its own strand relative to a second reference monomer on the other strand. Conversely, *n* has a negative value if a monomer is shifted toward the 3′-side of its own strand relative to a second reference monomer on the other strand.

■ ASSOCIATED CONTENT

Supporting Information

General experimental section; NMR spectra for new compounds; MS data for new modified ONs; representative T_m curves; additional thermal denaturation, UV−vis absorption, steady-state fluorescence emission, thermodynamic parameter, and dsDNA recognition data. The Supporting Information is available free of charge on the ACS Publications website at DOI: 10.1021/acs.joc.5b00742.

■ AUTHOR INFORMATION

Corresponding Author

*E-mail: hrdlicka@uidaho.edu. Tel: (208) 301-2616.

Notes

The authors declare no competing financial interest.

■ ACKNOWLEDGMENTS

This study was supported by award no. GM088697 from the National Institutes of General Medical Sciences, National Institutes of Health. Scholarships from the National Science Foundation under award no. 0648202 and the Department of Defense ASSURE (Awards to Stimulate and Support Undergraduate Research Experiences) Program (J.J.O.) are appreciated. We thank Dr. Alex Blumenfeld (Department of Chemistry, University of Idaho) and Dr. Lee Deobald (EBI Murdock Mass Spectrometry Center, University of Idaho) for assistance with NMR and mass spectrometric analysis and Prof. Carolyn Bohach (Food Science, University of Idaho) for access to gel documentation stations.

■ REFERENCES

(1) Besch, R.; Giovannangeli, C.; Degitz, K. *Curr. Drug Targets* **2004**, *5*, 691−703.
(2) Rogers, F. A.; Lloyd, J. A.; Glazer, P. M. *Curr. Med. Chem.: Anti-Cancer Agents* **2005**, *5*, 319−326.
(3) Ghosh, I.; Stains, C. I.; Ooi, A. T.; Segal, D. J. *Mol. BioSyst.* **2006**, *2*, 551−560.
(4) Nielsen, P. E. *Chem. Biodiversity* **2010**, *7*, 786−804.
(5) Mukherjee, A.; Vasquez, K. M. *Biochimie* **2011**, *93*, 1197−1208.
(6) Aiba, Y.; Sumaoka, J.; Komiyama, M. *Chem. Soc. Rev.* **2011**, *40*, 5657−5668.
(7) Vaijayanthi, T.; Bando, T.; Pandian, G. N.; Sugiyama, H. *ChemBioChem* **2012**, *13*, 2170−2185.
(8) Duca, M.; Vekhoff, P.; Oussedik, K.; Halby, L.; Arimondo, P. B. *Nucleic Acids Res.* **2008**, *36*, 5123−5138.
(9) Kaihatsu, K.; Janowski, B. A.; Corey, D. R. *Chem. Biol.* **2004**, *11*, 749−758.
(10) Dervan, P. B.; Edelson, B. S. *Curr. Opin. Struct. Biol.* **2003**, *13*, 284−299.
(11) Blackledge, M. S.; Melander, C. *Bioorg. Med. Chem.* **2013**, *21*, 6101−6114.
(12) Gaj, T.; Gersbach, C. A.; Barbas, C. F., III. *Trends Biotechnol.* **2013**, *31*, 397−405.
(13) Tse, W. C.; Boger, D. L. *Chem. Biol.* **2004**, *11*, 1607−1617.
(14) Hamilton, P. L.; Arya, D. P. *Nat. Prod. Rep.* **2012**, *29*, 134−143.
(15) Bentin, T.; Larsen, H. J.; Nielsen, P. E. *Biochemistry* **2003**, *42*, 13987−13995.
(16) Kaihatsu, K.; Shah, R. H.; Zhao, X.; Corey, D. R. *Biochemistry* **2003**, *42*, 13996−14003.
(17) Moreno, P. M. D.; Geny, S.; Pabon, Y. V.; Bergquist, H.; Zaghloul, E. M.; Rocha, C. S. J.; Oprea, I. I.; Bestas, B.; Andaloussi, S. E. L.; Jørgensen, P. T.; Pedersen, E. B.; Lundin, K. E.; Zain, R.; Wengel, J.; Smith, C. I. E. *Nucleic Acids Res.* **2013**, *41*, 3257−3273.
(18) Horne, D. A.; Dervan, P. B. *J. Am. Chem. Soc.* **1990**, *112*, 2435−2437.
(19) Filichev, V. V.; Nielsen, C. M.; Bomholt, N.; Jessen, C. H.; Pedersen, E. B. *Angew. Chem., Int. Ed.* **2006**, *45*, 5311−5315.
(20) Rusling, D. A.; Powers, V. E. C.; Ranasinghe, R. T.; Wang, Y.; Osborne, S. D.; Brown, T.; Fox, K. *Nucleic Acids Res.* **2005**, *33*, 3025−3032.
(21) Hari, Y.; Obika, S.; Imanishi, T. *Eur. J. Org. Chem.* **2012**, 2875−2887.
(22) Kutyavin, I. V.; Rhinehart, R. L.; Lukhtanov, E. A.; Gorn, V. V.; Meyer, R. B., Jr.; Gamper, H. B., Jr. *Biochemistry* **1996**, *35*, 11170−11176.

DOI: 10.1021/acs.joc.5b00742
J. Org. Chem. 2015, 80, 5395−5406

(23) Filichev, V. V.; Vester, B.; Hansen, L. H.; Pedersen, E. B. *Nucleic Acids Res.* **2005**, *33*, 7129−7137.
(24) Lohse, J.; Dahl, O.; Nielsen, P. E. *Proc. Natl. Acad. Sci. U.S.A.* **1999**, *96*, 11804−11808.
(25) Ishizuka, T.; Yoshida, J.; Yamamoto, Y.; Sumaoka, J.; Tedeschi, T.; Corradini, R.; Sforza, S.; Komiyama, M. *Nucleic Acids Res.* **2008**, *36*, 1464−1471.
(26) Demidov, V. V.; Protozanova, E.; Izvolsky, K. I.; Price, C.; Nielsen, P. E.; Frank-Kamenetskii, M. D. *Proc. Natl. Acad. Sci. U.S.A.* **2002**, *99*, 5953−5958.
(27) Sumaoka, J.; Komiyama, M. *Chem. Lett.* **2014**, *43*, 1581−1583.
(28) Rapireddy, S.; Bahal, R.; Ly, D. H. *Biochemistry* **2011**, *50*, 3913−3918.
(29) Bahal, R.; Sahu, B.; Rapireddy, S.; Lee, C.-M.; Ly, D. H. *ChemBioChem* **2012**, *13*, 56−60.
(30) Sander, J. D.; Joung, J. K. *Nat. Biotechnol.* **2014**, *32*, 347−355.
(31) Sau, S. P.; Kumar, T. S.; Hrdlicka, P. J. *Org. Biomol. Chem.* **2010**, *8*, 2028−2036.
(32) Sau, S. P.; Madsen, A. S.; Podbevsek, P.; Andersen, N. K.; Kumar, T. S.; Andersen, S.; Rathje, R. L.; Anderson, B. A.; Guenther, D. C.; Karmakar, S.; Kumar, P.; Plavec, J.; Wengel, J.; Hrdlicka, P. J. *J. Org. Chem.* **2013**, *78*, 9560−9570.
(33) Karmakar, S.; Guenther, D. C.; Hrdlicka, P. J. *J. Org. Chem.* **2013**, *78*, 12040−12048.
(34) Denn, B.; Karmakar, S.; Guenther, D. C.; Hrdlicka, P. J. *Chem. Commun.* **2013**, *49*, 9851−9853.
(35) Didion, B. A.; Karmakar, S.; Guenther, D. C.; Sau, S.; Verstegen, J. P.; Hrdlicka, P. J. *ChemBioChe.* **2013**, *14*, 1534−1538.
(36) Karmakar, S.; Madsen, A. S.; Guenther, D. C.; Gibbons, B. C.; Hrdlicka, P. J. *Org. Biomol. Chem.* **2014**, *12*, 7758−7773.
(37) (a) Crothers, D. M. *Biopolymers* **1968**, *6*, 575−584. (b) Tsai, C.; Jain, S. C.; Sobell, H. M. *J. Mol. Biol.* **1977**, *114*, 301−315. (c) Williams, L. D.; Egli, M.; Gao, Q.; Rich, A. In *Structure and Function, Vol. 1: Nucleic Acids*; Sarma, R. H., Sarma, M. H., Eds.; Adenine Press: Schenectady, NY, 1992; pp 107−125.
(38) Kumar, T. S.; Madsen, A. S.; Østergaard, M. E.; Sau, S. P.; Wengel, J.; Hrdlicka, P. J. *J. Org. Chem.* **2009**, *74*, 1070−1081.
(39) Andersen, N. K.; Anderson, B. A.; Wengel, J.; Hrdlicka, P. J. *J. Org. Chem.* **2013**, *78*, 12690−12702.
(40) Karmakar, S.; Anderson, B. A.; Rathje, R. L.; Andersen, S.; Jensen, T.; Nielsen, P.; Hrdlicka, P. J. *J. Org. Chem.* **2011**, *76*, 7119−7131.
(41) Matray, T. J.; Kool, E. T. *J. Am. Chem. Soc.* **1998**, *120*, 6191−6192.
(42) Kalra, N.; Babu, B. R.; Parmar, V. S.; Wengel, J. *Org. Biomol. Chem.* **2004**, *2*, 2885−2887.
(43) McGee, D. P. C.; Vaughn-Settle, A.; Vargeese, C.; Zhai, Y. *J. Org. Chem.* **1996**, *61*, 781−785.
(44) Abdel-Magid, A. F.; Carson, K. G.; Harris, B. D.; Maryanoff, C. A.; Shah, R. D. *J. Org. Chem.* **1996**, *61*, 3849−3862.
(45) Yamana, K.; Iwase, R.; Furutani, S.; Tsuchida, H.; Zako, H.; Yamaoka, T.; Murakami, A. *Nucleic Acids Res.* **1999**, *27*, 2387−2392.
(46) Nakamura, M.; Fukunaga, Y.; Sasa, K.; Ohtoshi, Y.; Kanaori, K.; Hayashi, H.; Nakano, H.; Yamana, K. *Nucleic Acids Res.* **2005**, *33*, 5887−5895.
(47) Christensen, U. B.; Pedersen, E. B. *Nucleic Acids Res.* **2002**, *30*, 4918−4925.
(48) Bryld, T.; Højland, T.; Wengel, J. *Chem. Commun.* **2004**, 1064−1065.
(49) Marin, V.; Hansen, H. F.; Koch, T. R.; Armitage, B. A. *J. Biomol. Struct. Dyn.* **2004**, *21*, 841−850.
(50) Dougherty, G.; Pilbrow, J. R. *Int. J. Biochem.* **1984**, *16*, 1179−1192.
(51) Asanuma, H.; Fujii, T.; Kato, T.; Kashida, H. *J. Photochem. Photobiol. C* **2012**, *13*, 124−135.
(52) Zinger, D.; Geacintov, N. E. *Photochem. Photobiol.* **1988**, *47*, 181−188.
(53) Manoharan, M.; Tivel, K. L.; Zhao, M.; Nafisi, K.; Netzel, T. L. *J. Phys. Chem.* **1995**, *99*, 17461−17472.
(54) Seo, Y. J.; Ryu, J. H.; Kim, B. H. *Org. Lett.* **2005**, *7*, 4931−4933.
(55) Østergaard, M. E.; Kumar, P.; Baral, B.; Guenther, D. C.; Anderson, B. A.; Ytreberg, F. M.; Deobald, L.; Paszczynski, A. J.; Sharma, P. K.; Hrdlicka, P. J. *Chem.—Eur. J.* **2011**, *17*, 3157−3165.
(56) Wilson, J. N.; Cho, Y.; Tan, S.; Cuppoletti, A.; Kool, E. T. *ChemBioChem* **2008**, *9*, 279−285.
(57) Bag, S. S.; Saito, Y.; Hanawa, K.; Kodate, S.; Suzuka, I.; Saito, I. *Bioorg. Med. Chem. Lett.* **2006**, *16*, 6338−6341.
(58) Asanuma, H.; Akahane, M.; Kondo, N.; Osawa, T.; Kato, T.; Kashida, H. *Chem. Sci.* **2012**, *3*, 3165−3169.
(59) Gupta, P.; Langkjær, N.; Wengel, J. *Bioconjugate Chem.* **2010**, *21*, 513−520.
(60) Karmakar, S. Ph.D. Dissertation, University of Idaho, January 2014.
(61) Mergny, J. L.; Lacroix, L. *Oligonucleotides* **2003**, *13*, 515−537.
(62) DNA hairpins were chosen as targets since alternatives, such as PCR fragments, cannot be readily used in electrophoretic mobility shift assays due to insufficient mobility differences between recognition complexes and unreacted targets (results not shown).
(63) Asseline, U.; Cheng, E. *Tetrahedron Lett.* **2001**, *42*, 9005−9010.
(64) Gottlieb, H. E.; Kotlyar, V.; Nudelman, A. *J. Org. Chem.* **1997**, *62*, 7512−7515.
(65) Dale, T. J.; Rebek, J., Jr. *J. Am. Chem. Soc.* **2006**, *128*, 4500−4501.
(66) Dioubankova, N. N.; Malakhov, A. D.; Stetsenko, D. A.; Gait, M. J.; Volynsky, P. E.; Efremov, R. G.; Korshun, V. A. *ChemBioChem* **2003**, *4*, 841−847.
(67) Astakhova, I. V.; Korshun, V. A.; Jahn, K.; Kjems, J.; Wengel, J. *Bioconjugate Chem.* **2008**, *19*, 1995−2007.

DOI: 10.1021/acs.joc.5b00742
J. Org. Chem. 2015, 80, 5395−5406